34th Annual International Conference of the IEEE EMBS
San Diego, California USA, 28 August - 1 September, 2012

Hermite Kernels for slice interpolation in medical images

Konstantinos K. Delibasis, Aristides I. Kechriniotis, Nicholas D. Assimakis, Simone Tassani and

George K. Matsopoulos

Abstract— **Univariate Hermite interpolation of the total degree (HTD) is an algebraically demanding interpolation method that utilizes information of the values of the signal to be interpolated at distinct support positions, as well as the values of its derivatives up to a maximum available order. In this work the interpolation kernels of the univariate HTD are derived, using several approximations of the 1st and 2nd order of discrete signal derivative. We assess the derived Hermite kernels in the task of medical image slice interpolation, against several other well established interpolation techniques. Results show that specific Hermite kernels can outperform other established interpolation methods with similar computational complexity, in terms of root mean square error (RMSE), in a number of interpolation experiments, resulting in higher accuracy interpolated images.**

I. Introduction

Interpolation is very frequently applied in signal and image processing, when it is required to calculate the value of an image at a spatial or temporal location with non-integer coordinates, in operations like resampling of signals and image geometric transformation or change of image pixelation. This work focuses on deriving the interpolation kernels from the univariate Hermite total degree (HTD) interpolation. We apply the derived kernels to slice interpolation in three-dimensional (3D) medical images. Biomedical imaging includes volume imaging in a slice by slice manner. In most clinical cases the voxel of the original 3D image is not cubic, due to required time for image acquisition and patient dosage concerns. However, many image processing applications (such as spatial image registration and visualization) require near isotropic image resolution in all directions. In these cases, three dimensional slice interpolation is applied [1]. HTD is one of the least explored interpolation methods and it utilizes the values of the function to be interpolated at a number of support points, as well as the values of its derivatives up to an arbitrary maximum order. More formally, the univariate HTD is described in the literature as following [2]: Let us assume that the value of a function $f(z)$ is given on n distinct, arbitrarily spaced support points $z_0, z_1, \ldots, z_{n-1}$. Let us assume further that the value of the derivatives of function f is also known on each of the interpolant points, up to the order of $m_0, m_1, \ldots, m_{n-1}$ respectively, where m_j a non-negative integer. If we denote the value of the derivative of function f of order i at point z_j as $f^{(i)}(z_j)=a_{ij}$, then there exists one and only one interpolating polynomial $r(z)$ of degree less than $\sum m_j$, such that $r^{(i)}\left(z_j\right)=a_{ij}$, $0\le j\le n\text{-}1$, $0\le i\le m_j\text{-}1$. This polynomial is explicitly given:

$$r(z)=\sum_{j=0}^{n-1}\sum_{i=0}^{m_j-1}\sum_{k=0}^{m_j-i-1} a_{ij}\frac{1}{i!}\frac{1}{k!}\left[\frac{\left(z-z_j\right)^{m_j}}{\Omega(z)}\right]_{z=z_j}^{(k)}\frac{\Omega(z)}{\left(z-z_j\right)^{m_j-i-k}}, \quad (1)$$

where $\Omega(z)=\prod_{j=0}^{n-1}\left(z-z_j\right)^{m_j}$. In this work, we derive the Hermit interpolation kernels using the interpolating polynomial (1) and test their performance in slice interpolation using 3D medical images, which is essentially treated as one-dimensional interpolation. The use of kernels in interpolation with equidistant support points has attracted considerable interest for signal interpolation ([3], [4], [5]) since it allows fast implementation of the interpolation method, as well as efficient execution. Especially for the HTD, given the relevant interpolation kernel, the implementation of the method becomes much easier and its application is also accelerated, since it becomes convolution-based. In [6] a number of Hermite interpolation kernels are derived up to 7th degree, by employing pairs of even and odd interpolation kernels. The values of the signal first derivative are calculated using an implicit scheme, based on IIR filtering, similar to the calculation of generalized interpolation coefficients as in [7] and [8]. Our work employs a single kernel irrespectively of the maximum order of signal derivative and achieves faster execution and smaller interpolation error.

II. Material and Methods

A. Derivation of kernels for HTD interpolation

Using the traditional, convolution-based formulation of signal interpolation (eq. (1) in [5]), the Hermite interpolating polynomial of (1) may be written as

Manuscript received March 15, 2012. This work was supported by the European Community, MOSAIC project (PIEF-GA- 2009-253924).

K.K. Delibasis is with the Department of Computer Science and Biomedical Informatics, University of Central Greece, Lamia, Greece (e-mail: kdelibasis@yahoo.com).

A. I. Kechriniotis and N. Assimakis are with the Department of Electronics, TEI of Lamia, Greece (e-mail: kechrin@teilam.gr , assimakis@teilam.gr).

S. Tassani and G.K. Matsopoulos are with the Institute of Communications and Computer Systems, National Technical University of Athens. National Technical University of Athens, 9 Iroon Polytechneiou str., 15780, Athens, Greece (e-mail: gmatso@esd.ece.ntua.gr).

Corresponding Author: S. Tassani, Institute of Communications and Computer Systems, phone: +30 210 772 3577; fax: +30 210 772 2468; e-mail: tassani.simone@ gmail.com.

$$r(z)=\sum_j a_{0j}K(z_j-z) \tag{2}$$

where $K(z)$ is the HTD interpolation kernel and a_{0j} is the 0th order derivative of the function to be interpolated at the jth support point, as defined as in (1). The $K(z)$ is usually a piecewise continuous and differentiable polynomial. Eq.(1) can be used to derive the family of Hermite interpolation kernels, under the following assumptions: a) the support points $z_0, z_1, \ldots, z_{n-1}$ are equidistant and b) the same maximum derivation order M is used for all support points, i.e. $m_0 = m_1 = \ldots = m_{n-1} = M+1$.

In order to express $r(z)$ in the form of (2), we have to approximate the i^{th} order signal derivative at j^{th} support position a_{ij} for $0 \le j \le n-1, 1 \le i \le M$ using finite differences. The proposed Hermite interpolation may be considered within the general osculatory interpolation scheme [9]. In this work, we utilized the approximations of derivatives of discrete signals given in [10] (assuming equidistant support positions) and we derive the Hermite kernels by expressing the Hermite interpolating polynomial of (1) in the form of (2). The accuracy of the derivative approximation depends on the number of signal points that are used. In the rest of the paper, we will indicate the Hermite kernels by a number of subscripts in the following order: the number of support points n, the maximum order of derivation M, the number of points for approximating the 1st derivative and the number of points for approximating the 2nd derivative (where applicable).

1) Cubic Hermite Kernel for n=2, M=1 using 2-point centered finite differences.

Since the number of support points is n=2, we may set $z_0 = 0, z_1 = 1$ without restricting generality. For M=1 (1st signal derivative), we followed an approach similar to [9] that tries to reconciliate (2) with $r(z)$ in (1). Using the 2-point centered finite differences for 1st derivative approximation $a_{10}=(a_{01}-a_{0,-1})/2$ and $a_{11}=(a_{02}-a_{00})/2$, the interpolating polynomial can be written as:

$$\begin{aligned} r(z) &= -\left(\frac{1}{2}z^3 - z^2 + \frac{1}{2}z\right)a_{0,-1} + \left(\frac{3}{2}z^3 - \frac{5}{2}z^2 + 1\right)a_{00} \\ &+\left(-\frac{3}{2}z^3 + 2z^2 + \frac{1}{2}z\right)a_{01} + \frac{1}{2}\left(z^3 - z^2\right)a_{02} \\ &= g_{-1}(z)a_{0,-1} + g_0(z)a_{00} + g_1(z)a_{01} + g_2(z)a_{02} \end{aligned}$$

The 4 polynomials g_{-1}, g_0, g_1 and g_2 of the above relation form the known Hermite cubic spline basis and they are defined for $z \in [0,1]$. By appropriately changing variable $z=z+1$ so that g_{-1} is defined in [1,2), $z=z-1$ so that g_2 is defined in (-2,-1], and $z=z-1$ so that g_1 is defined in [-1,0), we derive the following cubic Hermite kernel:

$$K_{2,1,2}(z) = \begin{cases} -\frac{1}{2}|z|^3 + \frac{5}{2}|z|^2 - 4|z| + 2, & 1 \le |z| < 2 \\ \frac{3}{2}|z|^3 - \frac{5}{2}|z|^2 + 1, & |z| < 1 \end{cases} \tag{3}$$

This kernel is identical to the 4-point cubic parametric kernel that is produced by setting its parameter to -0.5 in the Catmull Rom kernel ((23) in [4]), [11], which is optimal among cubic spline kernels [12].

2) Hermite Kernels with n=4, M=1

Let us consider the general case for n=4 support points and 1st derivative (M=1). In this case we may set $z_0 = -1, z_1 = 0, z_2 = 1$ and $z_3 = 2$, so that $z \in [0,1]$. The calculation of the 1st order derivative at the j^{th} support point is performed with up to 6-point central differences

$$a_{1,j} = c_1\left(a_{0,j+1} - a_{0,j-1}\right) + c_2\left(a_{0,j+2} - a_{0,j-2}\right) + c_3\left(a_{0,j+3} - a_{0,j-3}\right) \tag{4}$$

where $a_{0,j}$, $a_{1,j}$, is the value of the signal and its 1st derivative at the j^{th} support position as defined as in (1) and c_1, c_2, c_3 are parameters of the derivative approximation. If the 4-point central difference approximation is used for the 1st derivative, by setting $c_1 = 8/12, c_2 = -1/12, c_3 = 0$ in (4), according to [10], kernel $K_{4,1,4}$ is derived:

$$K_{4,1,4}(z) = \begin{cases} \frac{1}{432}|z|^7 - \frac{13}{216}|z|^6 + \frac{143}{216}|z|^5 - \frac{431}{108}|z|^4 + \frac{6145}{432}|z|^3 - \frac{6469}{216}|z|^2 & \\ -\frac{310}{9}|z| - \frac{50}{3} & 3 \le |z| < 4 \\ \frac{1}{432}|z|^7 - \frac{5}{216}|z|^6 - \frac{1}{216}|z|^5 + \frac{101}{108}|z|^4 - \frac{2111}{432}|z|^3 + \frac{2395}{216}|z|^2 & \\ -\frac{106}{9}|z| + \frac{14}{3} & 2 \le |z| < 3 \\ -\frac{19}{432}|z|^7 + \frac{31}{72}|z|^6 - \frac{317}{216}|z|^5 + \frac{61}{36}|z|^4 + \frac{365}{432}|z|^3 - \frac{59}{24}|z|^2 + 1, & 1 \le |z| < 2 \\ \frac{5}{48}|z|^7 - \frac{25}{72}|z|^6 - \frac{5}{24}|z|^5 + \frac{49}{36}|z|^4 + \frac{5}{48}|z|^3 - \frac{145}{72}|z|^2 + 1, & |z| < 1 \end{cases} \tag{5}$$

If we adopt the more accurate 6-point approximation of signal 1st derivative using c_1=3/4, c_2=-3/20, c_3=1/60 ([10], eq(4)), then kernel $K_{4,1,6}$ is derived:

$$K_{4,1,6}(z) = \begin{cases} -\frac{1}{2160}|z|^7 + \frac{11}{720}|z|^6 - \frac{463}{2160}|z|^5 + \frac{1193}{720}|z|^4 - \frac{2057}{270}|z|^3 + \frac{3749}{180}|z|^2 & \\ -\frac{94}{3}|z| + 20 & 4 \le |z| < 5 \\ -\frac{1}{240}|z|^6 + \frac{23}{240}|z|^5 - \frac{217}{240}|z|^4 + \frac{1073}{240}|z|^3 - \frac{1463}{120}|z|^2 + \frac{52}{3}|z| - 10, & 3 \le |z| < 4 \\ \frac{1}{80}|z|^7 - \frac{5}{24}|z|^6 + \frac{83}{60}|z|^5 - \frac{55}{12}|z|^4 + \frac{1817}{240}|z|^3 - \frac{113}{24}|z|^2 - \frac{22}{15}|z| + 2, & 2 \le |z| < 3 \\ -\frac{7}{144}|z|^7 + \frac{179}{360}|z|^6 - \frac{329}{180}|z|^5 + \frac{469}{180}|z|^4 - \frac{161}{720}|z|^3 - \frac{721}{360}|z|^2 + 1, & 1 \le |z| < 2 \\ \frac{7}{80}|z|^7 - \frac{3}{10}|z|^6 - \frac{5}{24}|z|^5 + \frac{49}{36}|z|^4 + \frac{7}{80}|z|^3 - \frac{77}{32}|z|^2 + 1 & |z| < 1 \end{cases} \tag{6}$$

3) Hermite Kernel with n=4, M=2

This family of kernels considers the 2nd order of signal derivatives as well. The position of the support points is given in the previous subsection. In addition to the 6-point approximation of 1st derivative used above, we employ up to 5-point approximation of 2nd derivative, using:

$$a_{2,j} = d_0 a_{0,j} + d_1\left(a_{0,j+1} + a_{0,j-1}\right) + d_2\left(a_{0,j+2} + a_{0,j-2}\right) \tag{7}$$

where the 1st subscript of a denotes the order of signal derivative and the 2nd subscript the support point index, as defined above and d_0, d_1, d_2 are parameters of the signal 2nd derivative approximation. We present the special case of the Hermite kernel with n=4, M=2 and $c_1 = 3/4, c_2 = -3/20, c_3 = 1/60$, $d_0 = -2, d_1 = 1, d_2 = 0$, thus using 6-point centred final difference approximation for the 1st derivative and 3-point centred final difference approximation for the 2nd derivative [10].

$$K_{4,2,6,3}=\begin{cases}\frac{11}{25920}|z|^{11}-\frac{559}{25920}|z|^{10}+\frac{107}{216}|z|^{9}-\frac{29323}{4320}|z|^{8}+\frac{532553}{8640}|z|^{7}-\frac{3364609}{8640}|z|^{6} & \\ +\frac{22633109}{12960}|z|^{5}-\frac{36016499}{6480}|z|^{4}+\frac{13284703}{1080}|z|^{3}-\frac{108149}{6}|z|^{2}+\frac{47210}{3}|z|-6200 & ,4\le|z|<5\\ -\frac{1}{144}|z|^{11}+\frac{87}{320}|z|^{10}-\frac{2759}{576}|z|^{9}+\frac{4009}{80}|z|^{8}-\frac{55329}{160}|z|^{7}+\frac{528671}{320}|z|^{6}-\frac{16053823}{2880}|z|^{5} & \\ +\frac{2124531}{160}|z|^{4}-\frac{7875787}{360}|z|^{3}+\frac{47471}{2}|z|^{2}-\frac{45770}{3}|z|+4400 & 3\le|z|<4\\ \frac{361}{8640}|z|^{11}-\frac{1007}{864}|z|^{10}+\frac{25019}{1728}|z|^{9}-\frac{30409}{288}|z|^{8}+\frac{160493}{320}|z|^{7}-\frac{468551}{288}|z|^{6} & \\ +\frac{31725857}{8640}|z|^{5}-\frac{4974481}{864}|z|^{4}+\frac{3313403}{540}|z|^{3}-\frac{12676}{3}|z|^{2}+\frac{25328}{15}|z|-296 & 2\le|z|<3\\ -\frac{215}{1728}|z|^{11}+\frac{26969}{12960}|z|^{10}-\frac{25777}{1728}|z|^{9}+\frac{258319}{4320}|z|^{8}-\frac{140669}{960}|z|7+\frac{972209}{4320}|z|^{6} & \\ -\frac{1837139}{8640}|z|^{5}+\frac{1483159}{12960}|z|^{4}-\frac{3667}{135}|z|^{3}-|z|^{2}+1 & 1\le|z|<2\\ \frac{1807}{8640}|z|^{11}-\frac{1259}{1080}|z|^{10}+\frac{2471}{1728}|z|^{9}+\frac{3551}{1440}|z|^{8}-\frac{5323}{960}|z|^{7}-\frac{583}{720}|z|^{6}+\frac{51521}{8640}|z|^{5} & \\ -\frac{2119}{4320}|z|^{4}-\frac{1111}{540}|z|^{3}-|z|^{2}+1 & |z|<1\end{cases} \quad (8).$$

B. *The slice interpolation problem*

Let us assume that a volume has been imaged and a three dimensional (3D) image has been acquired as a series of transverse images at different values of the Z axis, which we will call "slices". The problem of slice interpolation is defined as following [13]: given a number of slices at known equidistant positions along the Z axis, it is required to reconstruct the slice at an arbitrary Z coordinate. This is treated as a one-dimensional problem for each of the slice pixels and a number of convolution-based interpolation techniques are used to calculate the interpolated values ([4], [14], [15]). In order to quantitatively assess the accuracy of the Hermite interpolation kernels, we apply the kernels to interpolate a number of existing image slices and calculate the root mean squared error (RMSE) between the interpolated and the original slices [1]. For this reason, the 3D image I is subsampled along the Z direction by a factor N_{sub} of 2 or 3, as following: if a slice has index that is not an integer multiplier of N_{sub} then this slice is removed. In order to suppress the aliasing effect introduced by subsampling, we prefilter the ground truth data, as described in [16, p399], using a 20-point low pass FIR filter with normalized cut-off frequency equal to $0.99\,\pi/N_{sub}$.

C. *Computational complexity*

The Hermite interpolation in the case of 7th degree polynomial ((10), (11) in [6]) with 6th order of accuracy for the 1st derivative ((15) in [6]) requires 22 arithmetic operations per signal interpolation (two convolutions with 4-point kernels and the calculation of compact 1st order derivative using 4-point convolution (right side of [6, (15)]) and IIR filtering with one pair of reciprocal roots (left hand side of (15) in [6]). The proposed Hermite kernel $K_{4,2,6,3}(z)$ requires 20 arithmetic operations, whereas it utilises derivatives up to 2nd order and achieves substantially better RMSE than the 7th degree dual Hermite kernel of [6]. One may construct a Hermite kernel with M=3 following the technique described in our work, at the expense of increasing the degree of the polynomial, but with the same number of arithmetic operations as the $K_{4,2,6,3}(z)$ kernel, provided that the 3rd signal derivative is approximated with up to 6-point central differences. The number of arithmetic operations required for one signal value interpolation is shown for each interpolation method in the last column of Table II, assuming the use of look up tables for the kernel values.

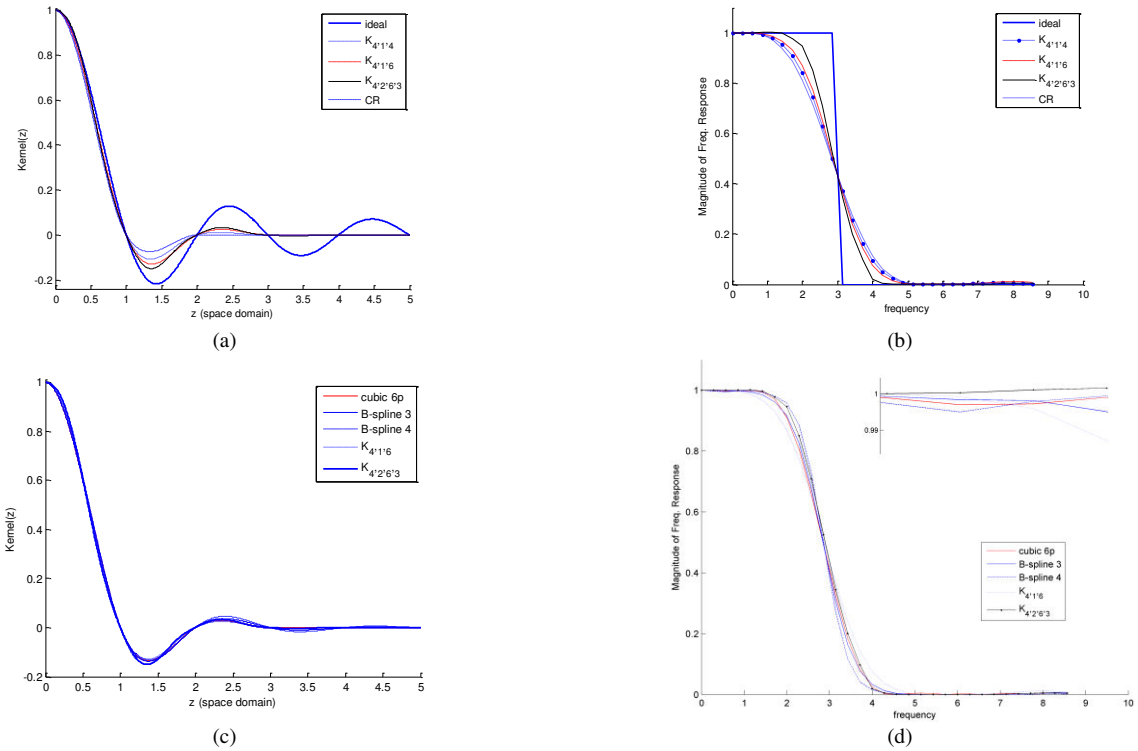

Figure 1. The proposed Hermite kernels and the reference kernels plotted in space (left column) and frequency domain (right column). In Fig. 1(d) the kernels' response in the pass band is shown in the zoomed inset, to assess response's flatness.

D. Assessing the properties of the Hermite kernels

The left column of Figure 1 shows the Hermite kernels as well as the other reference interpolation kernels in the time domain, whereas the right column plots the interpolation kernels in the frequency domain. Since the interpolation kernels are even functions, only the part for the non-negative independent variable is plotted. It can be observed (Fig 1a, 1b) that the $K_{4,2,6,3}$ kernel exhibits better characteristics than $K_{4,1,6}$ and $K_{4,1,4}$. All 3 Hermite kernels have more flat pass band and narrower transition band than the 4-point cubic kernels -CR (Fig 1b). The 6-point cubic interpolation kernel appears to exhibit marginally narrower transition band than the $K_{4,1,6}$ kernel, but it is clearly outperformed by the proposed $K_{4,2,6,3}$ Hemite kernel. As it can be observed in Fig. 1d the proposed $K_{4,2,6,3}$ kernel clearly outperforms the 3rd degree b-spline kernel, whereas in comparison to the 4rth degree b-spline interpolation, the proposed $K_{4,2,6,3}$ kernel exhibits more flat frequency response in the pass band and marginally less narrow transition band (see zoomed inset of the curves in Fig. 1d). The $K_{4,1,6}$ kernel is outperformed by both the B-spline kernels. These characteristics are compatible with the numerical results.

TABLE I. THE 3D MEDICAL DATA USED IN THIS STUDY

MODALITY / ANATOMY	LINES X COLUMNS X SLICES	BITS/ VOXEL	INTERSLICE DISTANCE (MM)
MRI Head	256x256x128	16	1.2
CT Chest	512x512x107	8	3
CT Foot	125x255x183	8	0.13

E. Data and interpolation experiments

Results are presented from a variety medical imaging data sets and interpolation experiments that are described in Table I, The data are acquired by computer assisted tomography (CT) of the foot [19] and thorax, as well as Magnetic Resonance Imaging (MRI) of the head [19]. No special pre-processing has taken place, except for the antialiasing filtering for subsampling, as described above. For each dataset, we set up two interpolation experiments, by setting the slice subsampling factor N_{sub} equal to 2 and 3. Results are averaged over 10 slices from each data set.

A number of established interpolation techniques were selected to compare against the Hermit interpolation kernels: the Lagrange kernel [14] for 4 and 6 support positions, linear interpolation [12], 6-point cubic polynomial interpolation kernel (eq.(24) in [4]), the Catmull-Rom interpolation kernel (CR) [11], as defined in [18], identical to K_{212} in (3) and the Mitchell-Netravali kernel (MN), defined in [4, (26)] for b=c=1/3. From the B-spline family of generalized convolution interpolation [7], [8] we selected degree 3 and 4, since the later has similar computational complexity with the proposed $K_{4,2,6,3}(z)$ kernel. We have also included the 7th degree Hermite kernel with 6th order first derivative from [6], since this was reported as the best performing Hermite kernel in that study.

III. EXPERIMENTAL RESULTS AND DISCUSSION

Table II shows the performance of the derived Hermite interpolation kernels in comparison to the other interpolation methods, in terms of RMSE, for all interpolation experiment. The number of arithmetic operations required for one signal value interpolation is also shown.The lowest RMSE in each experiment is depicted in bold. The interpolation RMSE was greatest for the experiments involving the MRI dataset, since it carried 16bits / voxel (see Table I).

As expected, the $K_{4,6,3,2}$ kernel outperforms the other Hermite kernels, since it employs 2nd order signal derivatives, with accurate approximation. Similarly, the $K_{4,1,6}$ kernel outperforms the $K_{4,1,4}$. The $K_{4,1,6}$ kernel, although it utilizes only the 1st order derivative of the signal, is very competitive among the non-generalized interpolation techniques. The proposed Hermite kernel $K_{4,6,3,2}$ outperforms all reference kernels in terms of RMSE in all experiments, except for the 4th degree B-spline. Both the proposed $K_{4,6,3,2}$ kernel and the 4th degree B-spline achieve best performance in half of the experiments. One could increase the order of the signal derivative when constructing the Hermite kernel, without increasing its computational complexity, assuming that a look up table is used for the calculation of the values of the kernel. However, the degree of the kernel would also increase.

TABLE II. RMSE ACHIEVED BY THE DERIVED HERMITE KERNELS AND THE OTHER METHODS IN COMPARISON, FOR ALL INTERPOLATION EXPERIMENTS.

METHOD		CT CHEST		MRI		CT-FOOT		NUM OF OPERATIONS
		N_{sub}=2	N_{sub}=3	N_{sub}=2	N_{sub}=3	N_{sub}=2	N_{sub}=3	
LAGRANGE	4-point	17.129	22.591	129.19	173.64	3.905	4.985	8
	6-point	16.712	21.995	125.68	170.41	3.695	4.833	12
LINEAR	2-point	19.457	24.335	140.39	184.26	4.566	5.484	2
CUBIC POLYNOMIAL INTERP	6-point	16.658	21.580	123.73	168.13	3.575	4.725	12
	4-point MN	18,240	23.337	133.35	177.99	4.156	5.192	8
	4-point CR	17.530	22.547	129.19	172.99	3.905	4.952	8
HERMITE KERNELS	$K_{4,1,4}$	17.028	21.999	126.08	170.08	3.719	4.818	8
	$K_{4,1,6}$	16.725	21.573	124.14	168.39	3.602	4.719	12
	$K_{4,2,6,3}$	16.548	21.510	123.33	**167.40**	**3.355**	**4.692**	20
B-SPLINE	deg. 3	16.564	21.494	123.41	168.12	3.545	4.712	10
	deg. 4	**16.278**	**21.168**	**121.32**	167.52	3.434	4.699	18
HERMITE [6]	deg. 7, 6th order 1st deriv	17.291	22.319	126.12	172.34	3.822	4.991	22

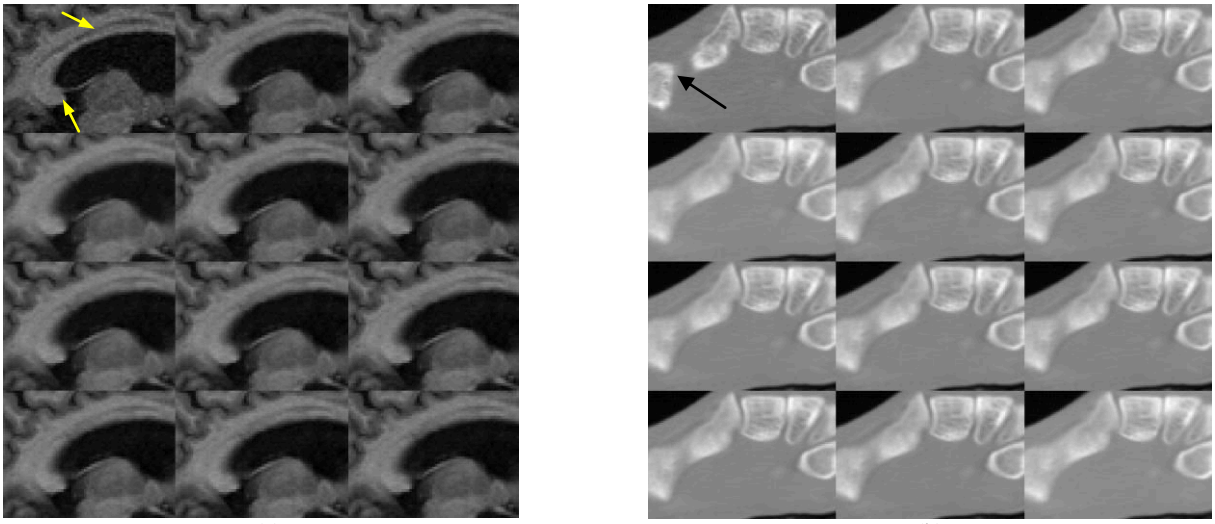

(a) (b)

Figure 2. The interpolation results for a random slice from (a) MRI N_{sub}=3 and CT Foot N_{sub}=3 (b). The images are arranged from left to right as follows: 1st row: Original image, proposed $K_{4,2,6,3}$, $K_{4,1,6}$, 2nd row: Linear, $K_{4\_1\_4}$, cubic 4p (CR), 3rd row: Lagrange 4p, Lagrange 6p, Cubic 6p, last row B-spline deg 3, B-spline deg 4, Hermite kernel deg=7 [6].

Figure 2 presents the interpolation results for a portion of a random transverse slice of the MRI study with N_{sub}=3 (a) and CT/Foot with N_{sub} =3 (b), for each of the interpolation methods. The RMSE values seem to correlate well with the observed reconstruction of fine image details. For instance the artifact that appears in all methods in Fig.2(b), marked by the arrow, is less extensive and less obvious in the case of $K_{4,2,6,3}$ kernel. Small image details, which appear to be more accurately reconstructed with the proposed $K_{4,2,6,3}$ kernel are also marked in Fig.2(a). Thus, the proposed kernel based on Hermite interpolation, presents an alternative interpolation technique, computationally almost equally expensive with the B-splines method that has the potential to prove useful for slice interpolation in 3D medical images.

ACKNOWLEDGMENT

CT foot and MRI head data sets were obtained from the Open Access Series of Imaging Studies (OASIS) project, supported by NIH grants P50 AG05681, P01 AG03991, P20 MH071616, RR14075, RR 16594, U24 RR21382, the Alzheimer's Association, the James S. McDonnell Foundation, the Mental Illness and Neuroscience Discovery Institute, and HHMI. The CT chest data set has been provided by the University General Hospital Attikon, Athens, Greece, courtesy of Dr. V. Kouloulias.

REFERENCES

[1] G. J. Grevera and J. K. Udupa, An Objective Comparison of 3-D Image Interpolation Methods, *IEEE Trans. Med. Imag*, vol. 17(4), pp. 642 – 652, 1998.

[2] I.S. Berezin, N.P. Zhidkov, *Computing method*, Pergamon, 1973 (Transl. from Russian, Chapter 8, Section 9).

[3] L. Liang, "Image Interpolation by Blending Kernels," *IEEE Signal Processing Letters*, vol.15, pp.805–808, 2008.

[4] T. M. Lehmann, Survey: Interpolation Methods in Medical Image Processing, *IEEE Trans. Med. Imag.*, 18(11) (1999) 1049 – 1075.

[5] T. Blu, P. Thevenaz, M. Unser, "Complete Parameterization of Piecewise-Polynomial Interpolation Kernels," *IEEE Trans on Image Processing*, vol. 12(11), pp. 1297-1309, 2003.

[6] Ryo Seta, Kan Okubo and Norio Tagawa, Digital Image Interpolation Method Using Higher-Order Hermite Interpolating Polynomials with Compact Finite-Difference, APSIPA Annual Summit and Conference, Japan 2009.

[7] M. Unser, A. Aldroubi and M. Eden, "B-spline signal processing: Part I – Theory," *IEEE TSP*, vol. 41(2), pp. 821 – 832, 1993.

[8] M. Unser, A. Aldroubi and M. Eden, "B-spline signal processing: Part I – Efficient Design and Applications," *IEEE TSP*, vol. 41(2), pp. 834 – 848, 1993.

[9] E. Meijering and M. Unser, A note on Cubic Convolution Interpolation, *IEEE TIP*, vol. 12(4), pp. 477 – 479, 2003.

[10] H. B. Keller, V. Pereyra, "Symbolic Generation of Finite Difference Formulas," *Mathematics of Computation,* 32(144), pp. 955-971, 1978.

[11] R. G. Keys, "Cubic convolution interpolation for digital image processing", *IEEE Trans. Acoust., Speech, Signal Processing*, vol. ASSP-29(6), pp. 1153–1160, 1981.

[12] S. Park, R. Schowengerdt, "Image reconstruction by parametric cubic convolution," *CVGIP*, vol. 23, pp. 258–272, 1983.

[13] C. Ciulla, *Improved Signal and Image Interpolation in Biomedical Applications: The Case of Magnetic Resonance Imaging (MRI)*, Medical Information science reference, Hershey New York.

[14] E.H.W.Meijering, W.J. Niessen, M.A. Viergever, "Quantitative evaluation of convolution-based methods for medical image interpolation", *Med. Image Anal*., vol. 5, pp. 111–126, 2001.

[15] P. Thevenaz, T. Blu, M. Unser, "Interpolation revisited", *IEEE Trans. Med. Imag*. vol. 19, 739–758, 2000.

[16] T. Blu, P. Thévenaz, and M. Unser, "Image interpolation and resampling", in Isaac Blankman (Ed.) Handbook of Medical Imaging, Processing and Analysis, Academic Press, pp393 – 423, 2000.

[17] J. D. Faires and R. L. Burden, Numerical Methods, Boston, MA: PWS, 1993.

[18] E. Catmull, R. Rom, A class of local interpolating splines, in R. E. Barnhill and R. F. Riesenfeld (Eds), Computer Geometric Design, pp. 317-326, Academic Press, New York, 1974.

[19] Open Access Series of Imaging Studies (OASIS), http://www.oasis-brains.org/app/template/Index.vm